Application-oriented analysis of material interface reconstruction algorithms in time-varying bijel simulations

Submission ID: 1054

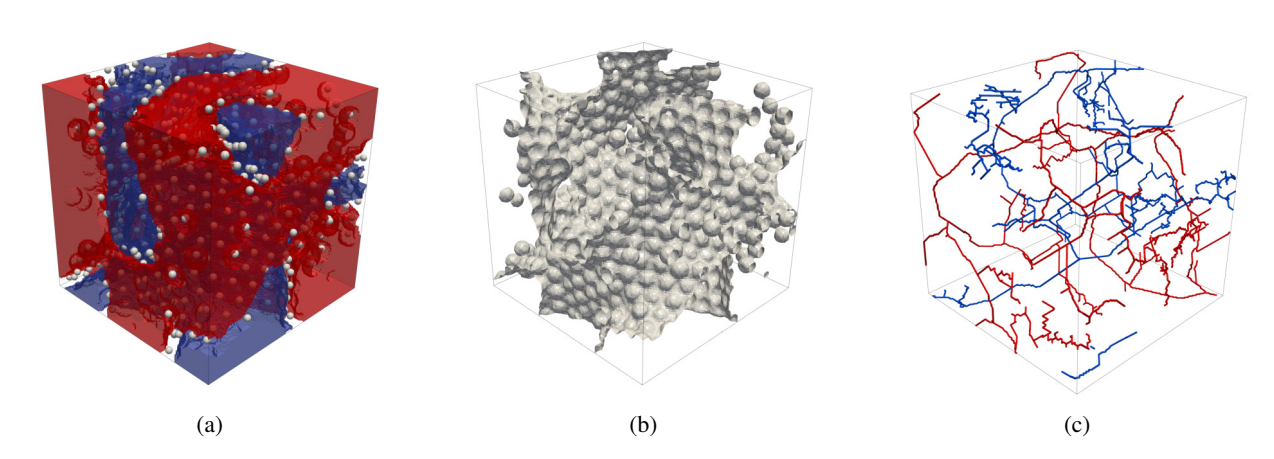


Figure 1: A multimaterial dataset is typically represented by a multivariate function defined on the cells of a cubical grid. In this paper, we use a bijel simulation dataset composed of oil and water with the addition of particles animated with the fluid to study the fluid-particle interactions. (a) Cells of the discrete domain can either contain oil (red), water (blue), or a mix of the two. Particles in the simulation, depicted as gray spheres, influence the formation of the bijel. Multimaterial interface reconstruction is a well-known problem in multimaterial analysis which involves \mathcal{M} (b) Identifying the surface separating the two materials. To analyze the characteristics of a multimaterial domain scientists need geometric structures beyond the interface. One of these is the medial axes, (c) here representing the topological skeletons of the oil (red) and water (blue) components.

Abstract

Multimaterial interface reconstruction has been investigated over the years both from a visualization and analytical point of view using different metrics. When focusing on visualization, interface continuity and smoothness are used to quantify interface quality. When the end-goal is interface analysis, metrics closer to the physical properties of the material are preferred (e.g., curvature, tortuosity). In this paper, we re-evaluate three Multimaterial Interface Reconstruction (MIR) algorithms, already integrated in established visualization frameworks, under the lens of application-oriented metrics. Specifically, we analyze interface curvature, particle-interface distance, and medial axis-interface distance in a time-varying bijel simulation. Our analysis shows that the interface presenting the best visual qualities is not always the most useful for domain scientists when evaluating the material properties.

CCS Concepts

• Computing methodologies → Volumetric models; • Human-centered computing → Scientific visualization;

1. Introduction

An important component of multi-material simulation analysis is the computation of its interface. Intuitively, reconstructing a multimaterial interface means to construct a surface *M* that separates materials within each cell of the domain. Studying the shape, topology, and cavities of the interface allows to derive important information

about the material under study [MTB*19]. To this end, Material Interface Reconstruction (MIR) algorithms has received a considerable amount of attention in computational physics [Cam21], computer graphics [AGDJ08], scientific visualizations [AGDJ10], and material science [WLWH12].

However, approaches developed by different communities have been evaluated with different criteria. Broadly speaking, we can classify MIR techniques as either simulation-oriented or visualization-oriented. The firsts focus on the physical properties such as mass convergence and volume conservation [NP17]. The seconds focus on the quality of the produced mesh [OCHJ12], or memory consumption and run time performance [MC10].

This paper provides two novelties in the analysis of MIR algorithms. First, we provide an application-oriented evaluation of several MIR algorithms integrated in existing scientific visualization frameworks (e.g., Visit [Chi12], ParaView [Aya15]). Second, we analyze the results consistency by considering the full time-varying evolution of the surface rather than a single time step.

2. Background and Related Work

Multimaterial analysis generally starts from a *simulation method* used to create a discrete multimaterial description. In this work we used a *Lattice Boltzmann Method (LBM)*, a relatively new simulation technique that can be seen as a mixture of particle-based (e.g., Lagrangian [GM77]), and mesh-based approaches (e.g. Eulerian [TP03]). LBM is often used in porous media simulations due to its ability to capture complex boundaries, and microscopic interactions [JH11]. The output of a LBM model is a multivariate function $f: \mathcal{D} \longrightarrow \mathbf{R}$, defined on the cells of a cubical grid \mathcal{D} .

Given f, Multimaterial Interface Reconstruction (MIR) is to compute a mesh \mathcal{M} describing the material boundaries. Ideally, we subdivide each cell of \mathcal{D} such that the total volume of each material within the cell equals the materials volume fraction. The difference between the original materials volume fraction and the volumes obtained by subdividing the cell according to $\mathcal M$ defines the volume fraction accuracy [MC10]. The most straightforward way to reconstruct the interface from f is by isocontouring [JH11, RST16, MTB*19]. In a two-material scenario [MC10] this means computing an isosurface within cells that have 0.5 volume fraction for each material. Since isocontouring can produce gaps and artifacts, especially on domains with more than two materials, the Simple Line Interface Calculation (SLIC) method [NW76] was introduced, which uses a moving window around each cell to fill the gaps left by the contour extraction. In the 2D case, gaps are filled up by either a horizontal or vertical plane.

To improve the geometric quality of the reconstructed interface, Piecewise Linear Interface Calculation (PLIC) methods generalize the SLIC approach by allowing lines/planes with arbitrary orientations defined based on the finite-difference on the volume fraction grid [HN81], the gradient of the volume fraction grid [You84], or by solving a least square problem [Puc91]. SLIC and PLIC methods have the advantage of speed and simplicity. The drawback is that they compute independent geometries for each material, which are generally disconnected, and reconstructing an interface with correct topology is a challenging problem [MC10, AGDJ10]. Meredith

et al. [Mer05,MC10] addressed this problem by averaging fractions on cell corners and intersecting the cell edges where the material fractions are equal. Anderson et al. [AGDJ08, AGDJ10] introduced the idea to subdivide cells based on the material fractions. This approach can guarantee bounded errors for the reconstructed surface but has the disadvantage of being memory and time-consuming.

Higher-order approaches have also been investigated like the agorithm by Prilepov et al. [POD*13] which presents a gradient-based method capable of capturing complex interface topology [POD*13]. More recently, a higher-order method was proposed which constructs cumulative integrals with nth-order B-splines over the interface [Cam21]. Like other methods focusing on synthetic data [OS88, Kaz13] this approach is computationally too complex to be usable on real scientific simulations yet.

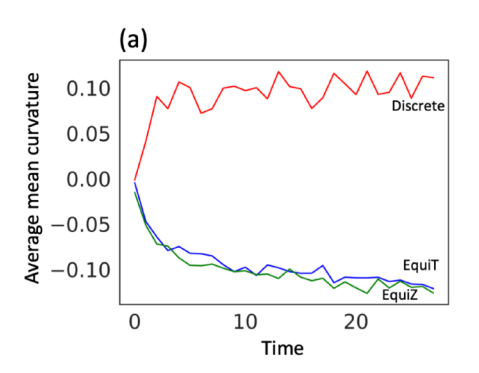
3. MIR Algorithm comparison

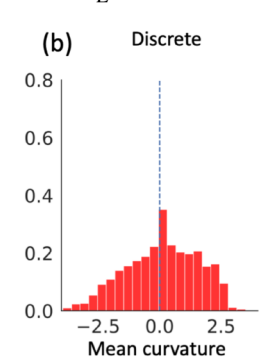
We compare three MIR algorithms widely adopted in the visualization community, namely, EquiT and EquiZ both proposed by Meredith et al. [Mer05], and Discrete proposed by Anderson et al. [AGDJ08]. All these methods are implemented in the VisIt framework. Notice that PLIC [You84] is provided by both Paraview [Aya15] and VisIt [Chi12]. Here we do not include PLIC in our analysis since it does not provide an interface as output. The evaluation uses a time-varying simulation of a bicontinuous interfacially jammed emulsion gel [JH11]. Volume fraction data are produced for 28 snapshots taken periodically for every 10⁵ time steps in a 256³ cube (see Figure 1a). Since Discrete required more than 64GB of memory (the limit for our system) to reconstruct the interface on the original dataset, we cropped the original dataset at its center within a 128³ window. The interface quality is evaluated using four different metrics related to geometric characteristics of the multimaterial [JH11, MTB*19], namely interface's Gaussian and Mean curvature, particles to interface distance, and medial axis to interface distance.

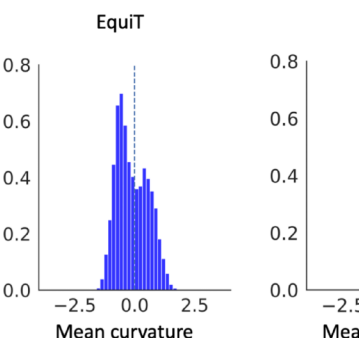
3.1. Evaluating interfaces with curvature estimators

Surface curvature is the most broadly used property in mesh quality estimation. Surface curvatures are defined based on two principal curvatures, k_1 and k_2 , which indicate how the surface bends in the two principal directions at that point. The Gaussian curvature is defined as the product of the two principal curvatures, while Mean curvature is the average value of the two [HEZ*19, Por94]. Gaussian and Mean curvature values are generally estimated at the vertices of a mesh [Por94]. This operation can be challenging in the presence of non-manifold vertices. In our evaluation, we used the approach proposed by Cohen et al. [CSM03], which estimates the curvature in a small neighborhood of a given vertex.

We computed Mean and Gaussian curvature on the interfaces extracted from all 28 snapshots by each of the three methods. For each interface, we analyzed the obtained curvature values by evenly sampling 10000 points on the interface. Bijels-derived structures captured the interest of material scientists due to their resemblance to minimal surface structures, which possess the optimal overall transport properties [GBB*09, LM10]. Ideally, a minimal surface structure should have zero Mean curvature and nega-







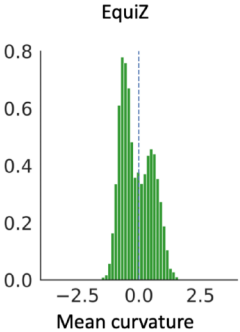


Figure 2: (a) Average Mean Curvature as a function of time. for Discrete (red), EquiT (blue), and EquiZ (green). (b) Mean Curvature distribution for a representative snapshot of the simulation.

tive Gaussian curvature. Thus, an ideal result from the analysis of the curvature for bijel interfaces should show similar average values [LM10, RST16].

Mean curvature analysis Figure 2a shows the average mean curvature value computed for each snapshot of the simulation. We can observe an early variation in the average Mean curvature. The phenomenon is due to drastic changes in the interface topology [JH11] that, after 2 snapshots, remains stable until the end of the simulation. We can notice that Discrete, EquiT, and EquiZ align differently to the expected results (average of Mean curvature equal to 0). The Discrete method is the only one with average Mean curvature above 0. Based on the curvature estimation in [CSM03], this indicates there are more convex polygons than concave polygons. Figure 2b shows the distribution of mean curvature values computed on the three interfaces for a representative snapshot (i.e., 10). These confirm the trends seen in Figure 2a since the Discrete method tends to have more positive values while EquiT, and EquiZ tend to have more negative values. Interestingly, Discrete produces a peak of vertices very close to 0 curvature which better aligns to the expected results [RST16]. On the other hand, EquiT and EquiZ show a bimodal distribution which suggests the reconstructed interface is smoother than the one produced by Discrete.

Gaussian curvature is very relevant for the analysis of bijels-derived structures. The average Gaussian curvature for a bijel is expected to be negative, indicating a hyperbolic surface in most of the regions [MTB*19,LM10,RST16]. Figure 3a shows the average Gaussian curvature values obtained on each snapshot for the three methods. We can notice that on average, only Discrete and EquiT produce overall negative values while the average Gaussian curvature of the interface computed by EquiZ assumes positive values. Interestingly, while EquiZ and EquiT both use a similar strategy to compute the interface, the tetrahedral-based subdivision used by EquiT seems beneficial for Gaussian curvature estimation.

Figure 3b shows a detailed view of the distribution of the Gaussian values using histograms, which confirms the general trends seen in the line chart. Notice that only a few values are obtained on the interface computed with the Discrete method since, similarly to SLIC [NW76], this approach reconstructs axis-aligned boundaries between voxels.

Overall, we should mention that curvature analysis presents challenges with all these methods due to small artifacts in the reconstructed interfaces. In the case of bijels analysis, this may come from contact points between spherical pockets corresponding to the original particles used by the simulation (see Figure 1b). From a domain scientist's perspective, this problem underlines the need for numerically robust, other than visually accurate, MIR algorithms.

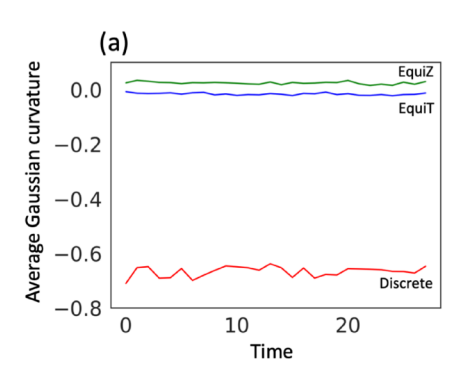
3.2. Evaluating interfaces with particle-surface distance

In bijel simulation, particle-interface contact angles describe how much energy is needed to detach a particle from the interface [JH11]. This is estimated by means of the particle-interface distance, which is computed by measuring the distance of each particle from the closest point on the interface.

Figure 4a shows the average distance values computed for each time step. We notice that the average particle distance increases over time, and the same trend is visible for all interfaces. However, we know particles should not detach from the interface since it is energetically unfavorable [JH11]. The hypothesis is that all these approaches are actually failing to capture thin interfaces formed around small droplets (particles) far away from the "main" interface. To test this hypothesis, we computed the number of expelled particles which is shown in Figure 4b. These are particles at distances more than twice the average particle-interface distance. From Figure 4b we notice that the number of such particles increases over time. Since particles are not being expelled [JH11], this suggests parts of the interface are being omitted. The results underline the challenge that all these approaches still have inaccurately reconstructed interfaces for small droplets.

3.3. Medial Axis and Material-Interface Distance

The medial axis [BLU67] is a topological skeleton, formed by edges and vertices, used to describe complex morphology. Medial axis is widely used in many areas, including path planning [WAS99], pattern recognition [SK05] and shape analysis [SCYW16]. In material science, the medial axis of a material volume is used to estimate physical properties of porous media such as domain size and tortuosity [MTB*19]. In the case of bijels analysis, we have two medial axes (one per material), and we are in-



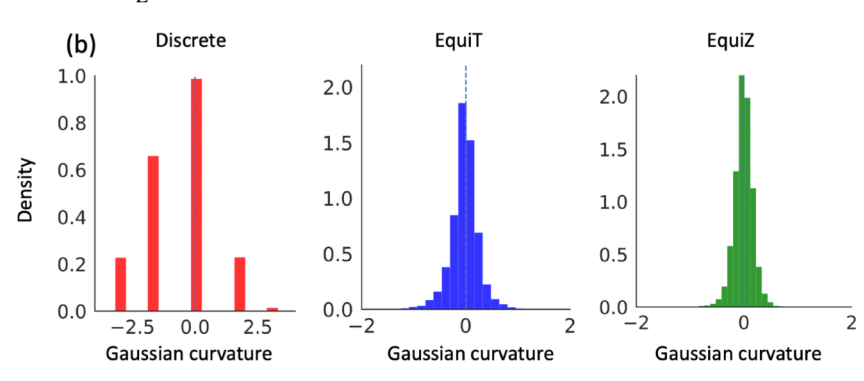


Figure 3: (a) Average Gaussian Curvature as a function of time for Discrete (red), EquiT (blue) and EquiZ (Green). (b) Gaussian Curvature distribution for a representative snapshot of the simulation.

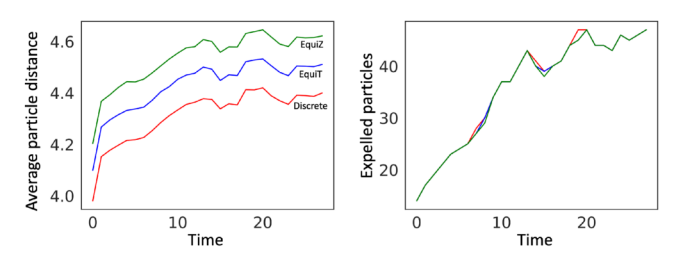


Figure 4: Average particle interface distance (a) and Expelled particle number (b) as a function of time with Discrete (red), EquiT (blue), and EquiZ (green). Each particle is classified as expelled particle if its distance from the interface is larger than twice the average particle-interface distance.

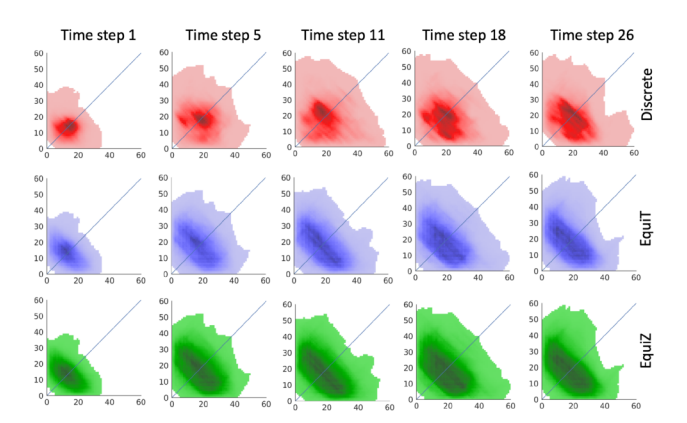


Figure 5: Co-variate distribution of the interface vertices distance from the two medial axis. For each density plot, X-axis represents the distance of a point in the interface from the medial axis of the oil material; Y-axis represents the distance of the point from the medial axis of the water material.

terested in investigating their relations with the interface extracted from each MIR algorithm. First, we compute the medial axis using the Teasar algorithm [SBB*00] on each material. Then, for each vertex on the interface, we compute its distance to the closest point in each medial axis.

Density plots in Figure 5 are generated from point clouds showing the co-variate distributions of the two material distances. Namely, each point corresponds to a vertex of the extracted interface. The coordinates of such points are defined by the distance of the interface's vertex from the medial axis computed from oil (Xaxis) and water (Y-axis). We can notice common patterns. Specifically, most points are concentrated close to the diagonal, indicating that most points in the reconstructed interfaces are equidistant from both medial axes. Also, the areas occupied by each density plot grow over time, indicating the interface is moving away from the medial axis (i.e., both material volumes are increasing). Before snapshot 16 the distance to the two medial axes is almost symmetrical. After snapshot 16, there is a noticeable decrease of bright pixels in the lower half of the plot, indicating that the interface is getting closer to the oil medial axis and away from the water medial axis. There are also noticeable differences across the three methods. Points created by Discrete are closer to the diagonal line compared to EquiT and EquiZ (i.e., denser regions in the density plots are concentrated closer to the diagonal). This indicates that Discrete is more likely to reconstruct interfaces equally distant from both medial axes.

4. Conclusion

In this paper, we compared three MIR algorithms in terms of interface curvature, particle-interface distance, and interface-material distance using a time-varying bijel simulation. From a qualitative point of view, EquiZ is considered the approach producing the best interfaces. However, we have shown that each approach presents strengths and weaknesses when evaluating the obtained interface from a quantitative point of view. Our results highlight the need to incorporate application-oriented evaluation metrics in MIR algorithms evaluation to improve MIR accuracy and to help domain scientists in the selection of the most suited MIR algorithm for their end-goal.

References

[AGDJ081 Anderson J. C., Garth C., Duchaineau M. A., Joy K. I.: Discrete multi-material interface reconstruction for volume fraction data. Computer Graphics Forum 27, 3 (May 2008), 1015-1022. doi:10.1111/j.1467-8659.2008.01237.x.2

- [AGDJ10] ANDERSON J. C., GARTH C., DUCHAINEAU M. A., JOY K. I.: Smooth, volume-accurate material interface reconstruction. *IEEE Trans. Visual. Comput. Graphics 16*, 5 (Sept. 2010), 802–814. doi: 10.1109/TVCG.2010.17.2
- [Aya15] AYACHIT U.: The ParaView guide: [a parallel visualization application]; updated for ParaView version 4.3\$nUtkarsh Ayachit. Kitware, 2015. 2
- [BLU67] BLUM, H.: A transformation for extracting new descriptors of shape. 362–380. 3
- [Cam21] CAMPBELL B. K.: An arbitrarily high-order three-dimensional cartesian-grid method for reconstructing interfaces from volume fraction fields. *Journal of Computational Physics* 426 (Feb. 2021), 109727. doi:10.1016/j.jcp.2020.109727.2
- [Chi12] CHILDS, HANK: VisIt: An end-user tool for visualizing and analyzing very large data. 2
- [CSM03] COHEN-STEINER D., MORVAN J.-M.: Restricted delaunay triangulations and normal cycle. In *Proceedings of the nineteenth conference on Computational geometry - SCG '03* (2003), ACM Press, p. 312. doi:10.1145/777792.777839.2,3
- [GBB*09] GOMMES C. J., BONS A.-J., BLACHER S., DUNSMUIR J. H., TSOU A. H.: Practical methods for measuring the tortuosity of porous materials from binary or gray-tone tomographic reconstructions. *AIChE J.* 55, 8 (Aug. 2009), 2000–2012. doi:10.1002/aic.11812.2
- [GM77] GINGOLD R. A., MONAGHAN J. J.: Smoothed particle hydrodynamics: theory and application to non-spherical stars. *Monthly Notices of the Royal Astronomical Society 181*, 3 (Dec. 1977), 375–389. doi:10.1093/mnras/181.3.375.2
- [HEZ*19] HSIEH M.-T., ENDO B., ZHANG Y., BAUER J., VALDEVIT L.: The mechanical response of cellular materials with spinodal topologies. *Journal of the Mechanics and Physics of Solids 125* (2019), 401–419. doi:10.1016/j.jmps.2019.01.002.2
- [HN81] HIRT C., NICHOLS B.: Volume of fluid (VOF) method for the dynamics of free boundaries. *Journal of Computational Physics 39*, 1 (Jan. 1981), 201–225. doi:10.1016/0021-9991(81)90145-5.
- [JH11] JANSEN F., HARTING J.: From bijels to pickering emulsions: A lattice boltzmann study. *Phys. Rev. E* 83, 4 (Apr. 2011), 046707. doi: 10.1103/PhysRevE.83.046707. 2, 3
- [Kaz13] KAZI, MICHAEEL MAJEED: Smooth Interface Reconstruction from Volume Fraction Data Using Variational Techniques and Level Set Methods. University of California, Berkeley, 2013. 2
- [LM10] LEE M. N., MOHRAZ A.: Bicontinuous macroporous materials from bijel templates. Adv. Mater. 22, 43 (Nov. 2010), 4836–4841. doi: 10.1002/adma.201001696. 2, 3
- [MC10] MEREDITH J. S., CHILDS H.: Visualization and analysisoriented reconstruction of material interfaces. *Computer Graphics Forum* 29, 3 (Aug. 2010), 1241–1250. doi:10.1111/j.1467-8659. 2009.01671.x. 2
- [Mer05] Meredith, JS: Material interface reconstruction in VisIt, 2005.
- [MTB*19] MCDEVITT K. M., THORSON T. J., BOTVINICK E. L., MUMM D. R., MOHRAZ A.: Microstructural characteristics of bijeltemplated porous materials. *Materialia* 7 (2019), 100393. doi:10. 1016/j.mtla.2019.100393. 2, 3
- [NP17] NGUYEN V.-T., PARK W.-G.: A volume-of-fluid (VOF) interface-sharpening method for two-phase incompressible flows. Computers & Fluids 152 (July 2017), 104–119. doi:10.1016/j.compfluid.2017.04.018.2
- [NW76] NOH W. F., WOODWARD P.: SLIC (simple line interface calculation). In Proceedings of the Fifth International Conference on Numerical Methods in Fluid Dynamics June 28 July 2, 1976 Twente University, Enschede, van de Vooren A. I., Zandbergen P. J., (Eds.), vol. 59.

- Springer Berlin Heidelberg, 1976, pp. 330–340. Series Title: Lecture Notes in Physics. doi:10.1007/3-540-08004-x_336. 2, 3
- [OCHJ12] OBERMAIER H., CHEN F., HAGEN H., JOY K. I.: Visualization of material interface stability. In 2012 IEEE Pacific Visualization Symposium (Feb. 2012), IEEE, pp. 225–232. doi:10.1109/PacificVis.2012.6183595. 2
- [OS88] OSHER S., SETHIAN J. A.: Fronts propagating with curvature-dependent speed: Algorithms based on hamilton-jacobi formulations. *Journal of Computational Physics* 79, 1 (Nov. 1988), 12–49. doi: 10.1016/0021-9991 (88) 90002-2. 2
- [POD*13] PRILEPOV I., OBERMAIER H., DEINES E., GARTH C., JOY K. I.: Cubic gradient-based material interfaces. *IEEE Trans. Visual. Comput. Graphics* 19, 10 (Oct. 2013), 1687–1699. doi:10.1109/TVCG.2013.16.2
- [Por94] PORTEOUS I. R.: Geometric differentiation: for the intelligence of curves and surfaces. Cambridge University Press, 1994. 2
- [Puc91] PUCKETT, ELBRIDGE GERRY: A volume-of-fluid interface tracking algorithm with applications to computing shock wave refraction. In Proceedings of the Fourth International Symposium on Computational Fluid Dynamics. 1991, pp. 933–938. 2
- [RST16] REEVES M., STRATFORD K., THIJSSEN J. H. J.: Quantitative morphological characterization of bicontinuous pickering emulsions via interfacial curvatures. Soft Matter 12, 18 (2016), 4082–4092. doi: 10.1039/C5SM03102H. 2, 3
- [SBB*00] SATO M., BITTER I., BENDER M., KAUFMAN A., NAKA-JIMA M.: TEASAR: tree-structure extraction algorithm for accurate and robust skeletons. In *Proceedings the Eighth Pacific Conference on Computer Graphics and Applications* (2000), IEEE Comput. Soc, pp. 281– 449. doi:10.1109/PCCGA.2000.883951.4
- [SCYW16] SUN F., CHOI Y.-K., YU Y., WANG W.: Medial meshes a compact and accurate representation of medial axis transform. *IEEE Trans. Visual. Comput. Graphics* 22, 3 (Mar. 2016), 1278–1290. doi: 10.1109/TVCG.2015.2448080.3
- [SK05] SEBASTIAN T. B., KIMIA B. B.: Curves vs. skeletons in object recognition. Signal Processing 85, 2 (Feb. 2005), 247–263. doi:10. 1016/j.sigpro.2004.10.016.3
- [TP03] TRAC H., PEN U.: A primer on eulerian computational fluid dynamics for astrophysics. *PUBL ASTRON SOC PAC 115*, 805 (Mar. 2003), 303–321. doi:10.1086/367747. 2
- [WAS99] WILMARTH S. A., AMATO N. M., STILLER P. F.: Motion planning for a rigid body using random networks on the medial axis of the free space. In *Proceedings of the fifteenth annual symposium on Computational geometry SCG '99* (1999), ACM Press, pp. 173–180. doi:10.1145/304893.304967.3
- [WLWH12] WEI L., LIN X., WANG M., HUANG W.: A cellular automaton model for a pure substance solidification with interface reconstruction method. *Computational Materials Science* 54 (Mar. 2012), 66–74. doi:10.1016/j.commatsci.2011.10.012.2
- [You84] YouNGS D.: An interface tracking method for a 3d eulerian hydrodynamics code. 2